Linking Lattice Strain and Fractal Dimensions to Non# monotonic Volume Changes in Irradiated Nuclear Graphite

Interdisciplinary Materials

WILEY

Interdisciplinary Materials Open Access

SHORT COMMUNICATION OPEN ACCESS

Linking Lattice Strain and Fractal Dimensions to Non-monotonic Volume Changes in Irradiated Nuclear Graphite

David J. Sprouster[1] | Sean Fayfar[2] | Durgesh K. Rai[2,3] | Anne Campbell[4] | Jan Ilavsky[5] | Lance L. Snead[1,2] | Boris Khaykovich[2]

[1]Department of Materials Science and Chemical Engineering, Stony Brook University, Stony Brook, New York, USA | [2]Nuclear Reactor Laboratory, Massachusetts Institute of Technology, Cambridge, Massachusetts, USA | [3]Current address: Mesoscale Atmospheric Process Lab, Earth Sciences Division, NASA Goddard Space Flight Center, Greenbelt, Maryland, USA | [4]Materials Science & Technology Division, Oak Ridge National Laboratory, Oak Ridge, Tennessee, USA | [5]X-ray Science Division, Advanced Photon Source, Argonne National Laboratory, Lemont, Illinois, USA

Correspondence: Boris Khaykovich (bkh@mit.edu)

Received: 23 February 2025 | **Revised:** 16 July 2025 | **Accepted:** 18 July 2025

Funding: This study was supported by the U.S. Department of Energy under Contracts (DE-AC02-06CH11357, DE-AC07-05ID14517, DESC0018322, IRP-22-27674).

Keywords: fractal dimensions | nuclear graphite | radiation damage | X-ray scattering

ABSTRACT

Graphite's resilience to high temperatures and neutron damage makes it vital for nuclear reactors, yet irradiation alters its microstructure, degrading key properties. We used small- and wide-angle X-ray scattering to study neutron-irradiated fine-grain nuclear graphite (Grade G347A) across varied temperatures and fluences. Results show significant shifts in internal strain and porosity, correlating with radiation-induced volume changes. Notably, porosity volume distribution (fractal dimensions) follows non-monotonic volume changes, suggesting a link to the Weibull distribution of fracture stress.

1 | Introduction

Graphite played a key role in nuclear reactors since the Chicago Pile and remains essential for current and next-generation designs like molten-salt and high-temperature gas reactors [1]. However, its complex irradiation response is unpredictable; the volume and other properties alter depending on graphite grade, irradiation temperature, and applied stress [2, 3]. Irradiated graphite first densifies—by up to 10%—then swells, with the turnaround point marking the volume minimum. A higher turnaround dose (in dpa) extends component lifespan, which is critical given disposal challenges. A predictive understanding of these effects is key to developing more durable graphite for safer, more economical nuclear energy.

Nuclear graphite has a composite-like structure of crystalline filler particles, less crystalline binder, pores, and cracks. Grains and pores exist in a variety of shapes and with a broad size distribution (sometimes between nanometers to micrometers). Radiation-induced changes in porosity and lattice stress drive the volume change and mechanical degradation [3–7]. The structural complexity and variability between nuclear graphite grades preclude reliable predictions of the irradiation response by molecular-dynamic simulations [8]. We provided a literature review in the Supporting Information focusing on relevant prior studies of microscopic properties and porosity.

The G347A graphite specimens investigated in this study were irradiated to fluences below and significantly above the

turnaround point across a broad temperature range. Synchrotron X-rays measurements were used to characterize structural changes across multiple length scales, from the interatomic (<1 nm) to mesoscopic scale (~10^4 nm).

The porosity of nuclear graphite is often described as fractal, which means that the pores' geometry looks similar over several orders of magnitude in length scale [9–11]. The self-similarity suggests uniformity in characteristics across a broad range of scales. The fractal dimension, D, characterizes the distribution of volume and surface area of pores [12, 13]. Small-angle X-ray scattering (SAXS) measures fractal dimensions directly [14, 15].

Fractal structures are common in materials like cement [16], rocks and minerals [17, 18], nanoparticle aggregates [19], and granular matter [20–23]. Fractal porosity has been used to explain the Weibull distribution of brittle fracture in ceramics and other porous materials [24, 25]. This paper is the first to suggest this framework for irradiated nuclear graphite [26, 27].

Our main finding is that the fractal dimensions closely follow the volume change curve vs irradiation damage, reaching a turnaround point near the volume turnaround and following similar temperature dependence. In addition, the crystallographic c-axis follows the same trend. These observations connect the morphology of pores with lattice strain, and potentially, the probability distribution of brittle fracture.

2 | Results

We measured irradiation-induced changes in lattice constants a and c (see Figures S1 and 1, together with the plot of the relative change in the total volume [3]). These results agree with previous measurements [4, 28, 29], except that the basal plane shrinkage ($\Delta a/a$) shows no signs of saturation. Williamson-Hall analysis [30] shows that the microstrain monotonically increases with the dose, in contrast to the nonmonotonic volume change. See Section S3 for details.

SAXS is ideal to study the effects of irradiation on the graphite porosity [11, 31, 32]. For SAXS, graphite is a two-component system, where pore surfaces are sharp interfaces that separate carbon and air, two components of different electronic scattering length densities (SLD). The SAXS results are modeled using power laws where the intensity $I(Q) \sim Q^{-\beta}$ and Q is the wavevector transfer. The value of β indicates the morphology of the structures within a material. Normally, $\beta = 4$ at large Q (Porod regime) in systems as diverse as polymers, microemulsions, and metallic alloys [33]. However, in nuclear graphite β was found to be a non-integer, a hallmark of fractality.

Fractal models were refined to SAXS measurements as described in the SI and displayed in Figure 2A,B. Our measurements only covered the region described by the surface fractal dimension (above ℓ). Due to the limited Q-range, we could not fit parameters ℓ and ξ. We fixed their values to those found previously [10], and set $D_m = D_s$. (Extending these measurements to lower Q requires X-ray tomography [10].) The unirradiated G347A graphite had a surface fractal dimension of $D_s = 2.6282(8)$ that increased in the irradiated samples as shown in Figure 2A,B.

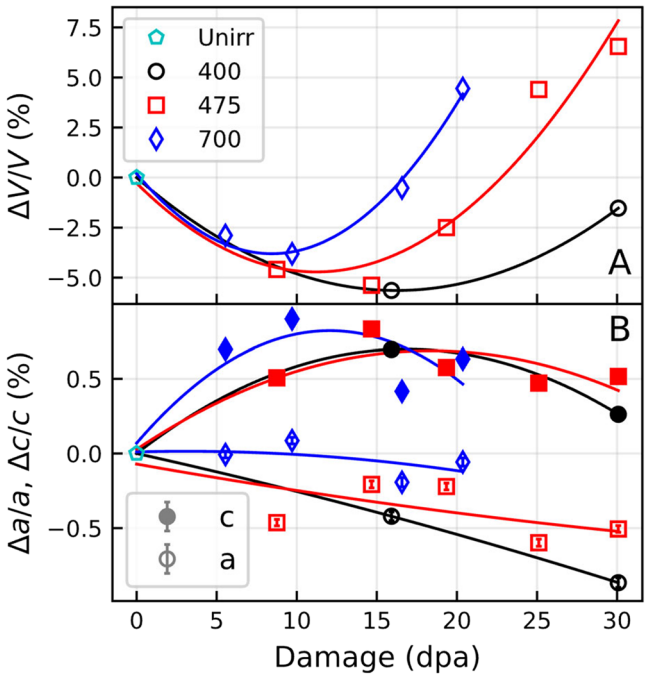

FIGURE 1 | Relative change in samples volume (A) and lattice constants (B) vs irradiation fluence measured in dpa. Shapes and colors denote different irradiation temperatures. Lines are quadratic fits of the data. (A) The volume change plot is from an earlier publication [3]. Blue diamonds: 700°C, red squares: 475°C, black circles: 400°C. The turnaround points are at the minima of the volume curves (~8, 12, and 16 dpa for 700, 475, and 400°C, respectively). (B) Filled and empty symbols denote c- and a-axis lattice parameters correspondingly. The colors and shapes correspond to the same temperatures as at the top graph. Error bars are smaller than the symbol size and can be seen inside the empty symbols.

Our most remarkable result is shown in Figure 3, the change of the fractal dimension with irradiation. Strikingly, D_s increases substantially and almost reaches the non-fractal value of $D_s = 3$ around the temperature-dependent turnaround point and decreases again at higher doses.

3 | Discussions

In a fractal distribution, the number of objects larger than a given size r, denoted $N(L > r)$, follows the relation $N \propto r^{-D}$, where D is the fractal dimension [13, 24]. If r_s is the size of the smallest crack (or pore), then the fraction F of cracks larger than r can be expressed as

$$F = \frac{N(L > r)}{N(L > r_s)} = \left(\frac{r}{r_s}\right)^{-D}. \quad (1)$$

Therefore, a higher fractal dimension indicates a greater proportion of smaller pores. According to our measurements, the fractal dimension increases upon densification and decreases with swelling due to the growth of larger pores. This picture

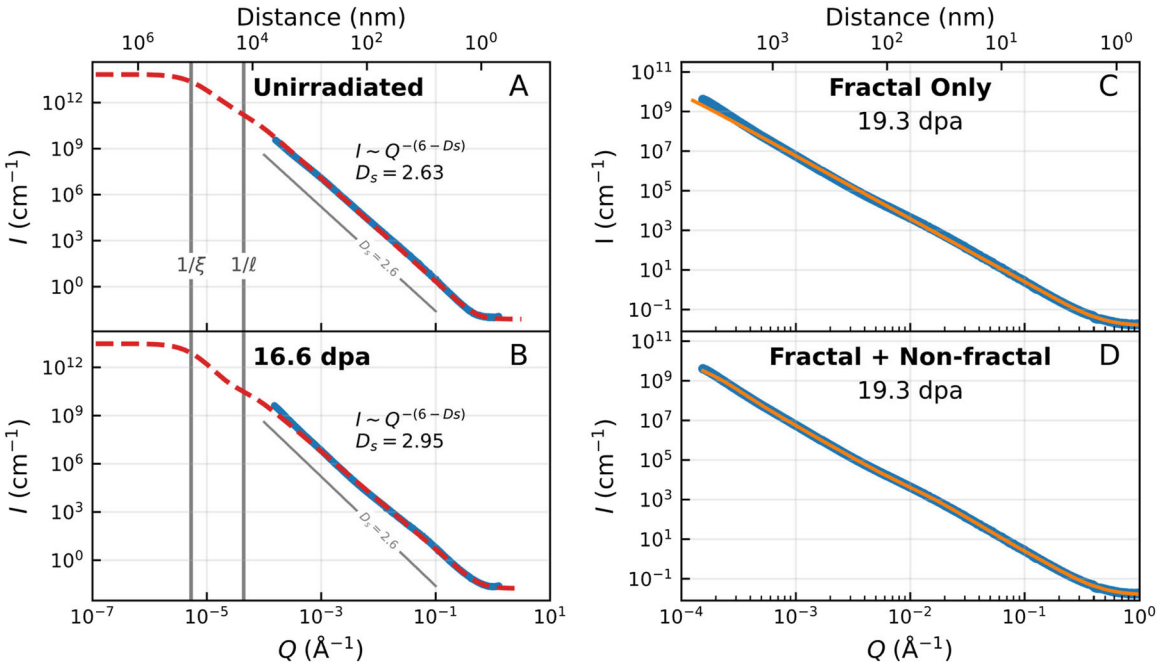

FIGURE 2 | SAXS measurements of G347A specimens fit to various models (The SLD contrast between carbon and air was calculated to be 15.26×10^{-6} Å^{-2}). Thick blue lines (data points) are the data; red dashed and orange lines are model fits. (A, B) The fractal model refined to the unirradiated and irradiated SAXS measurements shown with the length ℓ that separates the surface and mass fractal regions and the length ξ that separates the upper cutoff region. These scattering measurements only capture the surface fractal region. (C) SAXS of an irradiated specimen were fit using only a fractal model which fails to capture intensity at the lowest and mid-Q regions. (D) SAXS of the same irradiated specimen fit using a fractal model with the addition of two polydisperse spherical models for the non-fractal pores. Error bars (square root of X-ray counts) are too small to be visible.

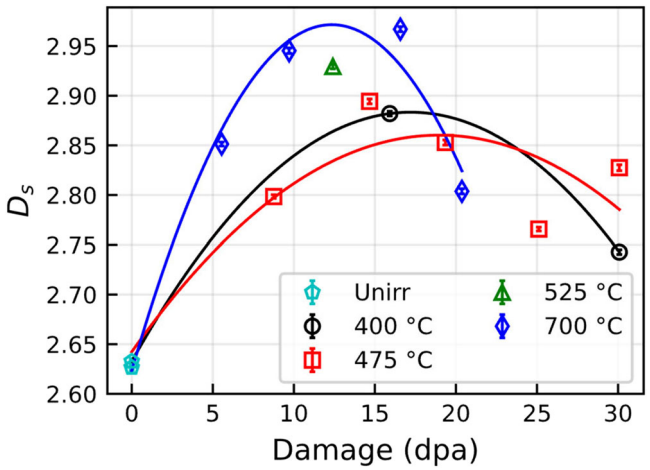

FIGURE 3 | The change in the surface fractal dimension with irradiation damage calculated from fitting the SAXS measurements. Error bars are visible inside the symbols; they are smaller than the symbols size.

implies that the fraction of larger pores in graphite decreases with increasing dpa below turnaround and increases above it.

Compacted granular matter exhibits analogous behavior, with the fractal dimension increasing alongside density under agitation, then decreasing as excessive agitation creates larger voids [22]. (Neutron irradiation is equivalent to agitation in that it supplies the energy to the system.) Drawing parallels between irradiated nuclear graphite and granular compaction may yield new insights into densification mechanisms.

A fractal-based model of nuclear graphite could enhance predictions of brittle fracture probability. This approach aligns with the Weibull distribution, which statistically attributes failure to the presence of critical flaws within a given volume [24–26]. A two-parameter Weibull distribution is the most frequently used:

$$F(\sigma_w) = 1 - \exp\left[-\left(\frac{\sigma_w}{\sigma_0}\right)^m\right], \tag{2}$$

where σ_w is the fracture stress, $F(\sigma_w)$ is the probability of failure of the stressed specimen, σ_0 and m are a scale factor and the Weibull modulus. According to the Griffith model [5], for cracks of radius r, the critical stress perpendicular to the crack plane $\sigma_w \propto r^{-1/2}$; then, Equations (1) and (2) lead to the Weibull modulus $m = 2D$, where D is the fractal exponent [24]. This model limits the Weibull modulus to $m \leq 6$, which is much smaller than normally quoted values [26, 27]. We speculate that the discrepancy can be removed by using the three-parameter distribution [24, 34]:

$$F(\sigma_w) = 1 - \exp\left[-\left(\frac{\sigma_w - \sigma_{w,th}}{\sigma_0}\right)^m\right],$$

where $\sigma_{w,th}$ is the threshold Weibull stress below which the fracture cannot occur [24]. To test this assertion, we will have

to replot existing graphite fracture distributions [26, 27] as three-parameter Weibull distributions. An interesting prediction of this model is that the Weibull modulus will change nonmonotonically with irradiation in accordance with Figure 3, with the largest Weibull modulus at around the turnaround point.

Future work will aim to directly link fractal dimensions with Weibull failure distributions. This could enable non-destructive estimation of Weibull moduli using SAXS or pore-quantifying methods like X-ray CT.

4 | Conclusions

The detailed analysis of the SAXS data in irradiated nuclear graphite shows that the pore size distribution near the turnaround point is markedly different from that of unirradiated and high-dose irradiated graphite. The fraction of larger voids decreases with increasing dose below turnaround and increases above it. We hypothesize that these porosity changes influence the Weibull fracture distribution, suggesting a potential for non-destructive estimation of Weibull parameters to assess graphite performance [24, 25, 34].

Acknowledgments

This study was supported by the U.S. Department of Energy, Office of Nuclear Energy under DOE Idaho Operations Office Contract DE-AC07-05ID14517 as part of Nuclear Science User Facilities award 16–651. This study used resources of the Advanced Photon Source, a U.S. Department of Energy (DOE) Office of Science user facility operated for the DOE Office of Science by Argonne National Laboratory under Contract No. DE-AC02-06CH11357. DJS and LLS acknowledge support from the U.S. Department of Energy Office of Fusion Energy Sciences under contract DESC0018322 with the Research Foundation for the State University of New York at Stony Brook. DJS, SF, and LLS acknowledge the Department of Energy Office of Nuclear Energy Integrated Research Project IRP-22-27674 for support. Graphite irradiations were performed at the Oak Ridge National Laboratory and sponsored by Tokai Carbon Co. Ltd. under the Material Science and Technology Division, Work-for-Others (WFO) Program, IAN: 16B630901, and DOE agreement: NFE-09-02345, with the U.S. Department of Energy. A portion of this study used resources at the High Flux Isotope Reactor a DOE Office of Science User Facility operated by the Oak Ridge National Laboratory. Open Access funding enabled and organized by MIT gold 2025.

Conflicts of Interest

The authors declare no conflicts of interest.

Data Availability Statement

The data that support the findings of this study are openly available in Zenodo at https://zenodo.org, reference number 10.5281/zenodo.13623346.

References

1. B. Zohuri, "Generation IV Nuclear Reactors." *Nuclear Reactor Technology Development and Utilization* (Elsevier, 2020), 213–246.

2. L. L. Snead, C. I. Contescu, T. S. Byun, and W. Porter, "Thermophysical Property and Pore Structure Evolution in Stressed and Non-Stressed Neutron Irradiated IG-110 Nuclear Graphite," *Journal of Nuclear Materials* 476 (2016): 102–109, https://doi.org/10.1016/j.jnucmat.2016.04.042.

3. A. A. Campbell, Y. Katoh, M. A. Snead, and K. Takizawa, "Property Changes of G347A Graphite Due to Neutron Irradiation," *Carbon* 109 (2016): 860–873.

4. G. B. Neighbour, "Modelling of Dimensional Changes in Irradiated Nuclear Graphites," *Journal of Physics D: Applied Physics* 33, no. 22 (2000): 2966–2972.

5. B. T. Kelly and T. D. Burchell, "Structure-Related Property Changes in Polycrystalline Graphite Under Neutron Irradiation," *Carbon* 32, no. 3 (1994): 499–505.

6. C. Karthik, J. Kane, D. P. Butt, W. E. Windes, and R. Ubic, "Neutron Irradiation Induced Microstructural Changes in NBG-18 and IG-110 Nuclear Graphites," *Carbon* 86 (2015): 124–131.

7. R. Krishna, J. Wade, A. N. Jones, M. Lasithiotakis, P. M. Mummery, and B. J. Marsden, "An Understanding of Lattice Strain, Defects and Disorder in Nuclear Graphite," *Carbon* 124 (2017): 314–333.

8. A. Chartier, L. Van Brutzel, and J. Pageot, "Irradiation Damage in Nuclear Graphite at the Atomic Scale," *Carbon* 133 (2018): 224–231.

9. Y. Vertyagina and T. J. Marrow, "Multifractal-Based Assessment of Gilsocarbon Graphite Microstructures," *Carbon* 109 (2016): 711–718.

10. Z. Zhou, W. G. Bouwman, H. Schut, et al., "From Nanopores to Macropores: Fractal Morphology of Graphite," *Carbon* 96 (2016): 541–547, https://doi.org/10.1016/j.carbon.2015.09.069.

11. Z. Mileeva, D. K. Ross, and S. M. King, "A Study of the Porosity of Nuclear Graphite Using Small-Angle Neutron Scattering," *Carbon* 64 (2013): 20–26.

12. P. Pfeifer and D. Avnir, "Chemistry in Noninteger Dimensions Between Two and Three. I. Fractal Theory of Heterogeneous Surfaces," *Journal of Chemical Physics* 79, no. 7 (1983): 3558–3565.

13. S. K. Sinha, "Scattering From Fractal Structures," *Physica D: Nonlinear Phenomena* 38, no. 1–3 (1989): 310–314.

14. J. Teixeira, "Small-Angle Scattering by Fractal Systems," *Journal of Applied Crystallography* 21, no. 6 (1988): 781–785.

15. P. W. Schmidt, "Small-Angle Scattering Studies of Disordered, Porous and Fractal Systems," *Journal of Applied Crystallography* 24, no. 5 (1991): 414–435, https://doi.org/10.1107/S0021889891003400.

16. M. A. Issa, M. A. Issa, M. S. Islam, and A. Chudnovsky, "Fractal Dimension—A Measure of Fracture Roughness and Toughness of Concrete," *Engineering Fracture Mechanics* 70, no. 1 (2003): 125–137.

17. L. M. Anovitz, G. W. Lynn, D. R. Cole, et al., "A New Approach to Quantification of Metamorphism Using Ultra-Small and Small Angle Neutron Scattering," *Geochimica et Cosmochimica Acta* 73, no. 24 (2009): 7303–7324, https://doi.org/10.1016/j.gca.2009.07.040.

18. J. Bahadur, Y. B. Melnichenko, M. Mastalerz, A. Furmann, and C. R. Clarkson, "Hierarchical Pore Morphology of Cretaceous Shale: A Small-Angle Neutron Scattering and Ultrasmall-Angle Neutron Scattering Study," *Energy & Fuels* 28, no. 10 (2014): 6336–6344, https://doi.org/10.1021/ef501832k.

19. A. Fabre, T. Steur, W. G. Bouwman, M. T. Kreutzer, and J. R. van Ommen, "Characterization of the Stratified Morphology of Nanoparticle Agglomerates," *Journal of Physical Chemistry C* 120, no. 36 (2016): 20446–20453.

20. G. R. McDowell, M. D. Bolton, and D. Robertson, "The Fractal Crushing of Granular Materials," *Journal of the Mechanics and Physics of Solids* 44, no. 12 (1996): 2079–2101.

21. A. R. Russell, "A Compression Line for Soils With Evolving Particle and Pore Size Distributions Due to Particle Crushing," *Géotechnique Letters* 1, no. 1 (2011): 5–9.

22. Y. Xu, "Fractal Dimension of Demolition Waste Fragmentation and Its Implication of Compactness," *Powder Technology* 339 (2018): 922–929.

23. D. L. Turcotte, "Fractals and Fragmentation," *Journal of Geophysical Research: Solid Earth* 91, no. B2 (1986): 1921–1926.

24. T. L. Anderson, "Application of Fractal Geometry to Damage Development and Brittle Fracture in Materials," *Scripta Metallurgica* 23, no. 1 (1989): 97–102.

25. A. Carpinteri, "Fractality of Scale-Invariant Cohesive Constitutive Laws." *Fracture and Complexity: One Century since Griffith's Milestone* (Springer Netherlands, 2021), 623–687, https://doi.org/10.1007/978-94-024-2026-5_11.

26. M. Srinivasan, "On Estimating the Fracture Probability of Nuclear Graphite Components," *Journal of Nuclear Materials* 381, no. 1–2 (2008): 185–198.

27. M. C. Carroll, W. E. Windes, D. T. Rohrbaugh, J. P. Strizak, and T. D. Burchell, "Leveraging Comprehensive Baseline Datasets to Quantify Property Variability in Nuclear-Grade Graphites," *Nuclear Engineering and Design* 307 (2016): 77–85.

28. R. H. Telling and M. I. Heggie, "Radiation Defects in Graphite," *Philosophical Magazine* 87, no. 31 (2007): 4797–4846.

29. L. L. Snead, T. D. Burchell, and Y. Katoh, "Swelling of Nuclear Graphite and High Quality Carbon Fiber Composite Under Very High Irradiation Temperature," *Journal of Nuclear Materials* 381, no. 1–2 (2008): 55–61.

30. G. K. Williamson and W. H. Hall, "X-Ray Line Broadening From Filed Aluminium and Wolfram," *Acta Metallurgica* 1, no. 1 (1953): 22–31.

31. W. T. Eeles, "Small-Angle X-Ray Scattering by Pile-Irradiated Graphite," *Nature* 188, no. 4747 (1960): 287–289.

32. D. G. Martin and J. Caisley, "Some Studies of the Effect of Irradiation on the Neutron Small Angle Scattering From Graphite," *Carbon* 15, no. 4 (1977): 251–255.

33. O. Glatter and O. Kratky, *Small Angle X-Ray Scattering* (Academic Press, 1982).

34. K. Rosahl, J. D. Booker, S. Lewis, and D. J. Smith, "A Statistical Approach for Transferring Fracture Events Across Different Sample Shapes," *Engineering Fracture Mechanics* 78, no. 1 (2011): 47–59.

Supporting Information

Additional supporting information can be found online in the Supporting Information section.
Supporting Table S1. Related to Table 1: List of samples, irradiation temperatures, radiation damage, and volume change. **Supporting Figure S1. Related to Figure 1:** X-ray diffraction patterns (Intensity vs. diffraction angle) of samples irradiated at different temperatures and fluences. **Supporting Figure S2. Related to Figure 2:** Williamson-Hall analysis as a function of irradiation dose at different temperatures in two crystallographic directions. **Supporting Figure S3. Related to Figure 3:** Fitting results of the log-normal distributions of the non-fractal pores.